

Detection of *Listeria monocytogenes* Using Luminol-Functionalized AuNF-Labeled Aptamer Recognition and Magnetic Separation

Weifeng Chen,[#] Liwei Cui,[#] Yanyan Song, Wei Chen, Yuan Su, Weidan Chang,^{*} and Wentao Xu^{*}



Cite This: *ACS Omega* 2021, 6, 26338–26344



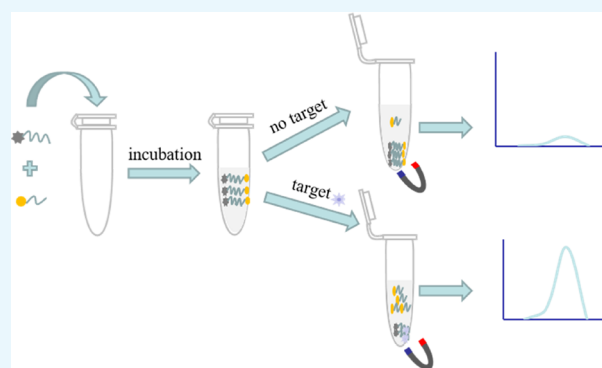
Read Online

ACCESS |

Metrics & More

Article Recommendations

ABSTRACT: A capture probe was constructed using a combination of magnetic Fe₃O₄ nanoparticles and an aptamer directed toward *Listeria monocytogenes*. A signal probe was prepared by combining luminol-functionalized flowerlike gold nanoparticles, obtained by combining luminol with chitosan bearing a complementary sequence of the aptamer. The complex consisting of the capture probe and signal probe could be removed through magnetic separation. Where the target was present within a sample, it competed with the complementary sequence for binding to the aptamer, causing a change of the chemiluminescent signal. The results indicated that a good linear relationship existed over the concentration range 1.0×10^1 – 1.0×10^5 CFU·mL⁻¹. It was established that it was feasible to use this approach to detect *L. monocytogenes* at levels as low as 6 CFU·mL⁻¹ in milk samples.



INTRODUCTION

At present, food safety has been widely concerned in the world. Food-borne diseases have become the main threat to human health, among which *Listeria monocytogenes* (*LM*) is one of the main food-borne pathogens that contaminate food worldwide. *LM* can contaminate all kinds of foods, especially foods rich in starch and protein, such as meat and meat products, poultry and egg products, milk and other dairy products. *LM* has strong vitality and can survive at 0–45 °C. It can still grow at the temperature of refrigerators, which is also an important characteristic of it that is different from other food-borne pathogens. *LM* can cause sepsis, meningitis, and mononucleosis in humans and animals, posing a great threat to the health of infants and the elderly who have poor immunity.^{1,2} Although there are regulations for the presence of *LM* in food, it is very widespread and monitoring of *LM* in food is regularly performed using microbiological analysis.³ Therefore, it is very important to establish a rapid and accurate detection approach for *LM*.⁴

Traditional culture methods rely on an initial culture, with subsequent biochemical and serological identification, the duration of which is at least 3 days. Nucleic acid sequence amplification-based methods, such as real-time fluorescence PCR, multiple PCR, and loop-mediated isothermal amplification (LAMP), are also widely used to detect *LM* due to their speed, efficiency, and simplicity.^{5–8} However, these methods require more than 10 h of bacterial culture and DNA extraction. In addition, various natural inhibitors in real-world biological and food samples, such as phenolic

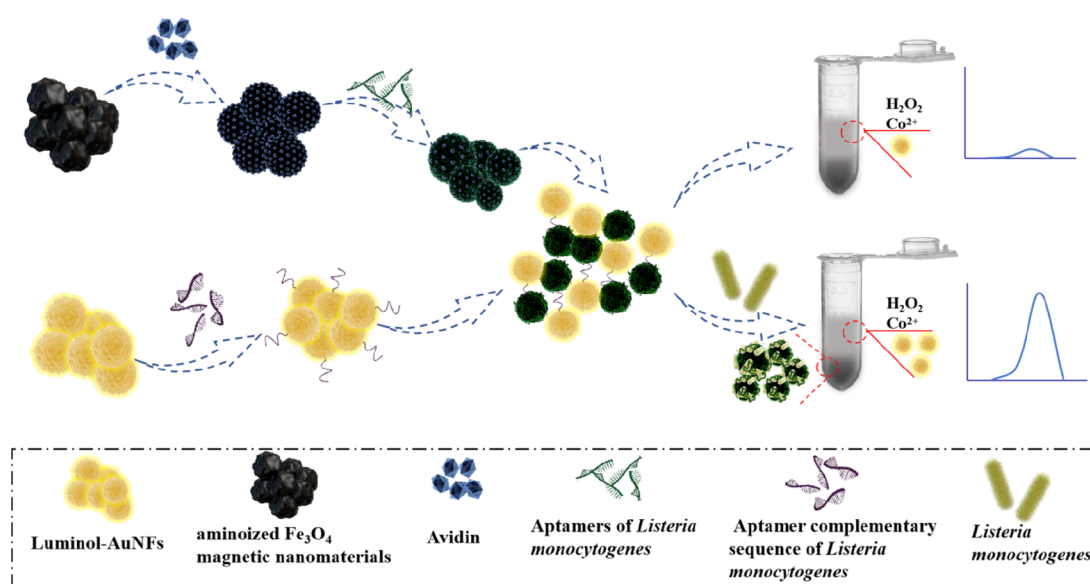
compounds, enzymes, fats, salts, and proteins, can reduce or inhibit amplification efficiency.⁹ Immunological assays, such as enzyme-linked immunosorbent assays, and immunofluorescence assays have also been used for the rapid detection of *LM*.^{10,11} However, the immunological assays require specific monoclonal antibodies, which have some disadvantages, such as requiring complex procedures, varying avidity, and low specificity. Despite the current development of genetically engineered antibodies, their avidity is far lower than that of monoclonal antibodies.¹² In recent years, a number of biosensors have been developed to detect *LM*. Electrochemiluminescence has attracted many researchers due to its high sensitivity, wide linear range, low background, and simple equipment usage. Furthermore, many improvements have been introduced to reduce the limit of detection and enhance its sensitivity.¹³ Luminol is a chemiluminescent reagent commonly used in chemiluminescence (CL) reaction systems with good luminescence efficiency. A popular CL reaction system involving the reaction of luminol and H₂O₂ has been widely developed for the detection of a variety of substances. Additionally, gold colloids in the form of nanoparticles have

Received: July 5, 2021

Accepted: August 18, 2021

Published: September 27, 2021



Scheme 1. Schematic Illustration of *LM* Detection Based on Luminol-AuNFs-Labeled Aptamer Recognition and Magnetic Separation

been found to enhance the CL of the luminol– H_2O_2 system.¹⁴ Aptamers selected from random oligonucleotide libraries based on SELEX technology consist of specific oligonucleotide sequences. They display numerous advantages compared with conventional antibodies, such as high stability, strong specificity, and convenient synthesis.¹⁵ They are currently widely used in the detection of various pathogenic bacteria, the diagnosis and treatment of diseases, and biosensor construction, in addition to other fields.¹⁶

To better solve the enrichment culture of pathogenic bacteria and determine the matrix effect of food samples, many upstream pre-separation and/or pre-concentration methods have been developed to solve the above problems, among which the methods based on magnetic nanoparticles are the most widely used. Magnetic nanoparticles exhibit high magnetic conductivity, excellent biocompatibility, biodegradability, and other beneficial properties and can combine with a variety of functional molecules, such as enzymes, antibodies, DNA, *etc.* Therefore, they could be expected to be widely used in targeted drugs, controlled release, enzyme immobilization, immune detection, DNA and cell separation and classification, among other fields.^{17–23} Based on the special properties of magnetic nanoparticles, many researchers mainly use their superparamagnetism to separate, enrich, and purify target substances in the process of detection of food-borne pathogens, which will effectively shorten the enrichment time, eliminate the influence of sample matrix on detection sensitivity, and greatly improve the detection efficiency.

In the present study, a highly sensitive and specific *LM* detection system was established based on the aptamer-linked biofunctional magnetic nanomaterial. In this system, the luminol-functionalized flowerlike gold nanoparticles (AuNFs) were used as chemiluminescent markers and magnetic nanoparticles connecting the ligand as a capture probe. First, the aptamer of *LM* was connected to magnetic nanoparticles to construct the capture probe. Second, the complementary sequence was connected with the luminol-functionalized AuNFs to construct the signal probe. When there was *LM* in the reaction system, the capture probe

preferentially bound to *LM* and the signal probe squeezed down from the capture probe (Scheme 1). Last, the sensitivity assay had a detection limit of up to $6 \text{ CFU}\cdot\text{mL}^{-1}$. Thus, this method has a good prospect in the detection of *LM* in complex foods.

RESULTS AND DISCUSSION

Schematic Diagram of the Detection of *LM* Based on Luminol-Functionalized Nanogold-Labeled Aptamers.

A schematic illustration of *LM* detection based on luminol-AuNFs-labeled aptamer recognition and magnetic separation is displayed in Scheme 1. Magnetic nanoparticles (MNPs) with ammonia on the surface were prepared using a two-step reduction method, with kinins modified to their surface by glutaraldehyde and subsequently connected to a biotinized aptamer to make capture probes. At the same time, the sulfhydryl aptamer complementary sequence was connected with the luminol nanomaterial to prepare a signal probe. When there is no target, the signal probe and the capture probe are connected by base complementation. Under a magnetic field, the signal probe in the supernatant decreases and the luminescence intensity is lower. The specific binding with the capture probe increases the number of signal probes in the supernatant and increases the luminescence intensity. There is a positive correlation between the target and the luminous intensity so as to realize the quantitative determination of the target.

Characterization of Luminol-Functionalized Nanogold. Luminol-functionalized AuNFs were synthesized by reduction of chloroauric acid with luminol and chitosan. Their growth mechanism is as follows: luminol and chitosan act as reductants to reduce chloroauric acid and act as protectants to protect the gold nanoparticles, but luminol has stronger reducing properties, so luminol first reduced chloroauric acid to a large number of nanoparticles.

Subsequently, the nanoparticles were aggregated into primary three-dimensional nanoparticles by attachment using a large number of amino groups in the chitosan macromolecule, while chitosan promoted secondary growth to obtain

strongly bound three-dimensional nanoflower-like macromolecules. The size of the nanoparticles decreased with increasing luminol concentration, and the size of the complete flower was determined by the quantity of chitosan. The lower the concentration of chitosan, the weaker its protective effect, and so the larger the size of the flower. The prepared material was characterized by transmission electron microscopy (TEM), as shown in Figure 1.

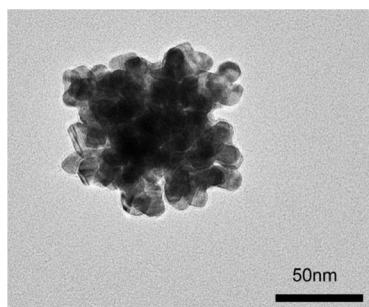


Figure 1. TEM image of the as-prepared luminol-AuNFs.

Characterization of the Steady-State CL System. The chemiluminescent properties of luminol-AuNFs were investigated by static injection. When 0.2 mol/L H_2O_2 was injected into the luminol-AuNFs, a strong transient luminescence signal occurred. The chemiluminescent principle can be briefly described as follows: under certain conditions, luminol can be oxidized by H_2O_2 to luminol-ox, and transient luminescence occurs when it transitions to an excited state. When H_2O_2 and Co^{2+} were added to the CL system, the intensity of the system will be significantly enhanced.

Characterization of Aminated Fe_3O_4 Magnetic Nanoparticles. X-ray diffraction (XRD) was used to analyze the crystal properties of the magnetic nanomaterials. The results suggested that the magnetic nanoscale Fe_3O_4 prepared in the present study conforms entirely to the standard card JCPDS 82-1533 and is consistent with the spinel Fe_3O_4 structure shown in Figure 2B. It was observed by infrared spectroscopy that the spectra of organosilylated nano- Fe_3O_4 (b) had an absorption peak representing Fe–O at approximately 583 cm^{-1} , an absorption peak representing Si–O at 1113 cm^{-1} , and an O–H stretching vibration at 3427 cm^{-1} , compared with the IR spectra of nano- Fe_3O_4 (a). Therefore, the results

established that a Si–OH layer was formed on the surface of the nanoscale ferric oxide by organosilylation. A comparison between (b) and (c) in Figure 2A demonstrates that a downward absorption peak at approximately 1623 cm^{-1} formed, indicating that the surface of the material had $-\text{NH}_2$ functional groups following amination, in addition to absorption peaks representing Si–O at approximately 1124 cm^{-1} and $-\text{CH}_3$ at around 2924 cm^{-1} . These coexisting functional groups demonstrate that the amino groups successfully attached to the surface of the nanomaterials.

Construction of the Signal Probe. The signal probe is a complex of the complementary sequence of the aptamer and luminol-functionalized AuNFs. The aptamer was attached to the gold nanoparticles via Au–S bonds. To improve ligation efficiency, tri-(2-carboxyethyl) phosphine (TCEP) was included in the ligation process. TCEP was able to break the S–S covalent bonds inside the mercapto-oligonucleotide sequence and between the two nucleotide sequences, facilitating Au–S bonding between the sulfhydryl nucleotides and gold nanoparticles. UV–vis scanning was performed on the original solution and the supernatant before and after binding of the mercapto-oligonucleotide sequence and the luminol-functionalized flower-shaped gold nanoparticle. As displayed in Figure 3, the absorbance at 260 nm of the complementary sequence

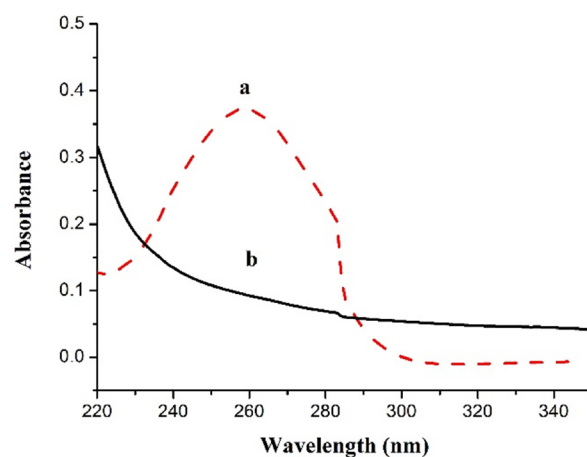


Figure 3. UV–vis absorption spectra of the (a) thiolated complementary sequence of LM aptamer and (b) supernatant after conjugation of the thiolated complementary sequence to the luminol-AuNFs.

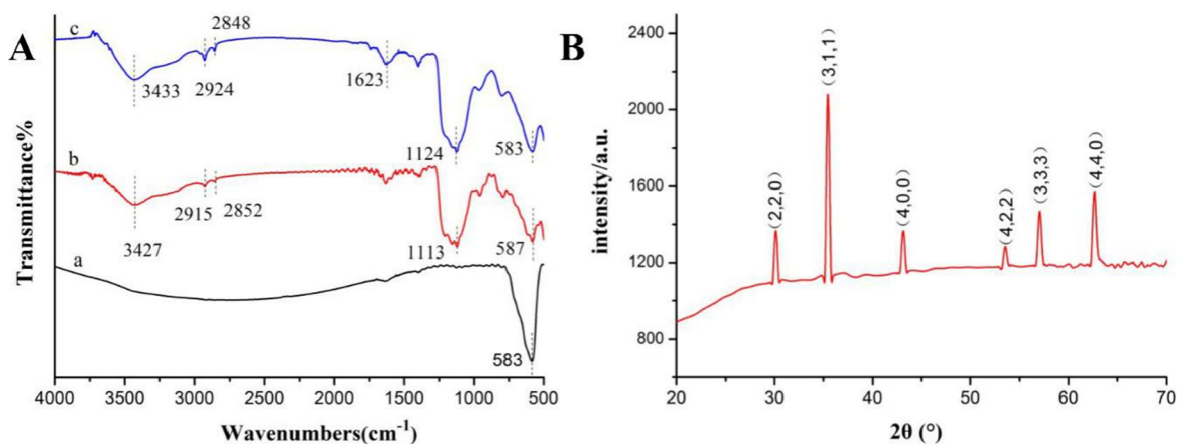


Figure 2. Characterization of magnetic Fe_3O_4 nanomaterials by (A) IR and (B) XRD.

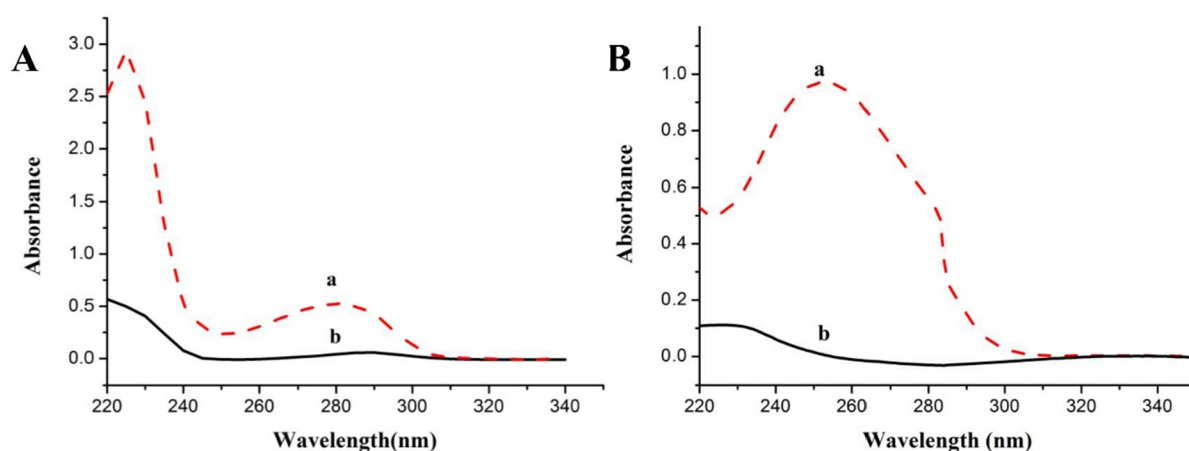


Figure 4. (A) UV-vis absorption spectra of (a) avidin and (b) supernatant after the conjugation of avidin to glutaraldehyde-modified MNPs. (B) UV-vis absorption spectra of (a) biotinylated aptamers of LM and (b) the supernatant after conjugation of biotinylated aptamers to the avidin-modified MNPs.

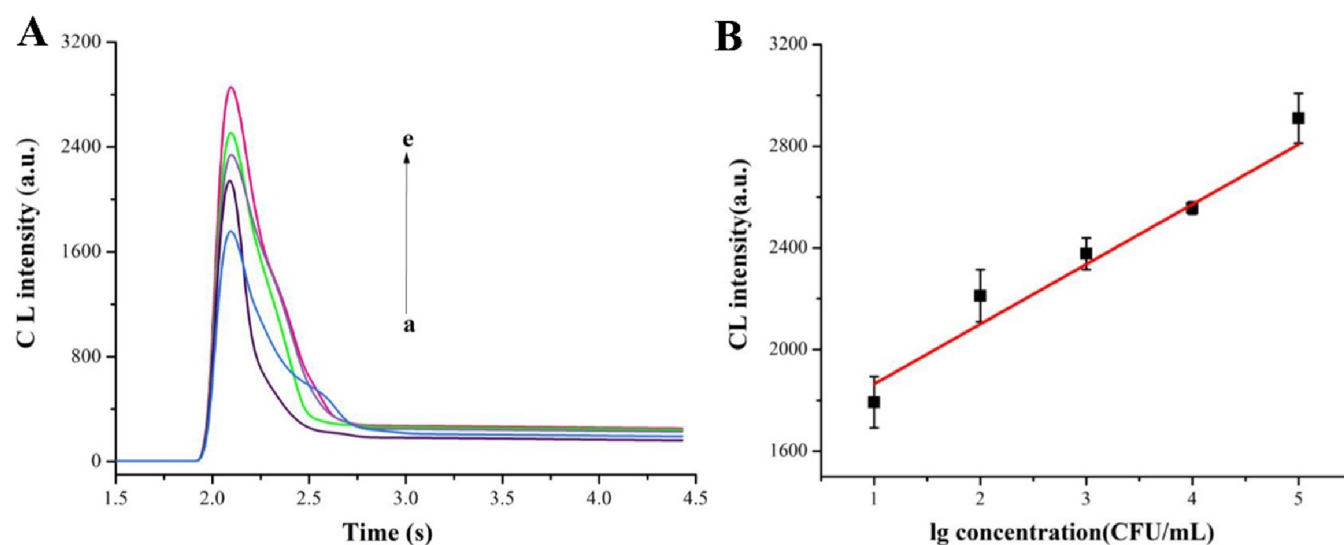


Figure 5. (A) CL responses for LM at the concentrations of (a) 1×10^1 , (b) 1×10^2 , (c) 1×10^3 , (d) 1×10^4 , (e) 1×10^5 CFU·mL⁻¹. (B) Linear curve for LM detection.

of the aptamer decreased significantly after incubation, indicating that it had been successfully attached to the surface of the luminol nanogold particles and that the signal probe was successfully connected.

Construction of the Capture Probe. Assembly of the capture probe is conducted as follows. In the first step, glutaraldehyde acted as a cross-linking agent to attach avidin to the aminoized magnetic nanoferric tetroxide. The amino group in the structure of the amino-modified MNPs was formalized by glutaraldehyde, after which the aldehyde groups on the nanomaterials were condensed with amino groups containing avidin to form a Schiff base. Finally, the avidin was combined with the surface of the nanomaterials. Because avidin is a protein, it has a characteristic absorption peak at 280 nm. The binding of avidin to the nanomaterials was indirectly determined by comparing the UV absorption values at 280 nm. First, the original avidin solution was added to the formylated magnetic nanomaterials via amino groups. After incubation, the collected supernatant and original solution of avidin were assessed using ultraviolet spectrophotometry. The ultraviolet measurements at a wavelength of 280 nm were

compared before and after incubation, as shown in Figure 4A. Using the same principle, the degree of combination of the aptamer and avidinized nanomaterials could be determined by absorption at a wavelength of 260 nm. The aptamer was added to the aminated magnetic nanomaterial modified by avidin. The supernatant collected after incubation and the original solution of the aptamer were tested in the same way by ultraviolet spectroscopy. As shown in Figure 4B, absorbance at 260 nm decreased significantly after incubation, indicating that some of the aptamers were attached to the surface of the magnetic nanomaterials modified by avidin, confirming that the captured probes were successfully prepared.

Analytical Performance. Different concentrations of LM were incubated with the capture and signal probes. When little or no LM was present in the system, only the signal probe was combined with the capture probe, and the chemiluminescent intensity of the supernatant system was minimal. When LM was present in the system, the bacteria competitively combined with and captured the signal probe, increasing luminescence of the supernatant. Figure 5A demonstrates continuously increasing CL signals as LM concentrations varied from $1 \times$

10^1 to 1×10^5 CFU·mL⁻¹. As shown in Figure 5B, the linear range for LM detection was 1×10^1 – 1×10^5 CFU·mL⁻¹. The limit of detection was estimated to be 6 CFU·mL⁻¹. Interestingly, the detection limit was similar to that reported for LM by Yang et al.²⁸ The regression equation is described by $Y = 1706 + 228.3x$, with a correlation coefficient of 0.949.

Specificity Assay. *Salmonella*, *Staphylococcus aureus*, *Bacillus subtilis*, *Escherichia coli*, and *Shigella flexneri* were selected to conduct specificity analysis. Figure 6 demonstrates that the chemiluminescent intensity caused by LM was considerably higher than that caused by the other five bacteria, indicating high specificity for this method.

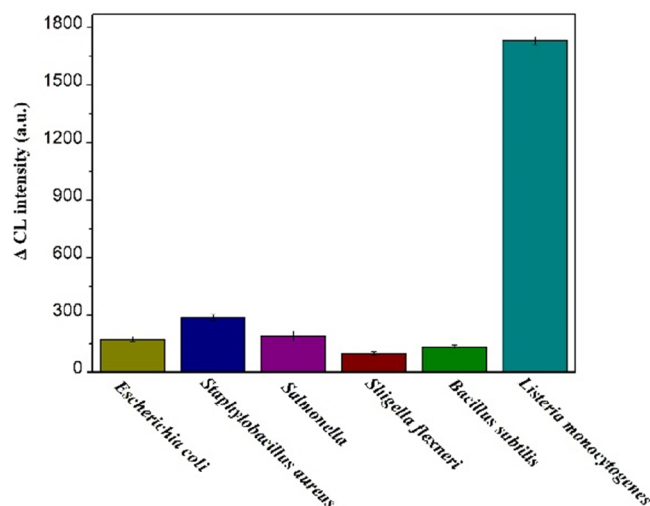


Figure 6. Specificity of the proposed method for LM detection. The concentrations of *E. coli*, *S. aureus*, *Salmonella*, *S. flexneri*, and *B. subtilis* were all 1.0×10^3 CFU·mL⁻¹.

To verify the reliability of this method in real-world samples, actual samples were prepared to evaluate standard addition recovery performance. Three concentrations of LM (1×10^1 CFU·mL⁻¹, 1×10^3 CFU·mL⁻¹, and 1×10^5 CFU·mL⁻¹) were added to milk samples, and then, the method was used to analyze LM concentration. The results listed in Table 1

Table 1. Recovery Tests of LM Spiked in Real Samples

sample	added (CFU·mL ⁻¹)	found (CFU·mL ⁻¹)	RSD (%)	recovery (%)
milk	1.0×10^1	1.1×10^1	2.9	110
	1.0×10^3	0.97×10^3	3.1	97
	1.0×10^5	0.91×10^5	5.8	91

indicate that the standard recovery of LM was from 1×10^1 CFU·mL⁻¹ to 1×10^5 CFU·mL⁻¹, with relative standard deviation (RSD) values between 2.9 and 5.8. The results indicate that the CL adaptor sensor constructed using this method accurately and reliably detected LM content in samples.

CONCLUSIONS

In this study, a facile CL method was developed for the detection of LM based on magnetic separation and luminol-AuNFs labeled-aptamer recognition. The proposed method in this study possesses the following advantages: (1) It shortens the testing time. The aptamers are easy to synthesize, which

can greatly reduce the cost and time of the detection process. By labeling the aptamers on magnetic nanomaterials, pathogens from food samples can be effectively and rapidly enriched, rendering this method a specific quantitative detection tool for direct detection of pathogens. (2) It has a wide detection range and a low detection limit. Within the concentration range of 1×10^1 to 1×10^5 CFU·mL⁻¹, a good linear relationship was observed between the change in CL intensity and the logarithm of the bacterial concentration, with a detection limit of 6 CFU·mL⁻¹. (3) It has high specificity. The cross-reaction test indicated that this method has adequate specificity to LM. (4) Applicability in food samples. When applying this method to milk samples, an acceptable recovery ranging from 91% to 110% with RSD values all below 5.9% was observed. In this experiment, luminol was used as a CL reagent. If we change it to a more sensitive CL reagent such as *N*-(4-aminobutyl)-*N*-ethyl isoluminol, the sensitivity of this method can be further improved. Collectively, the results above demonstrate that this method can accurately and reliably detect the content of LM in foods.

MATERIALS AND METHODS

Tri-(2-carboxyethyl)phosphine (TCEP, purity > 98.0%) was purchased from TCI Development Co., Ltd. (Shanghai, China). Avidin, chitosan, glutaraldehyde (25%), glacial acetic acid, nano-ferric oxide (20 nm), tetraethyl silicate (TEOS, 99.99%), and 3-aminopropyl triethoxysilane (APTS, 99.99%) were obtained from Aladdin Co., Ltd. (Shanghai, China). LM (ATCC19115), *E. coli* (CICC10389), *S. aureus* (CICC21600), *Salmonella* (CICC21482), *S. flexneri* (CMCC51302), and *B. subtilis* (CICC10732) were purchased from the China Center of Industrial Culture Collection (CICC). The aptamer sequence finally selected (5'-biotin-ATC CAT GGG GCG GAG ATG AGG GGG AGG AGG GCG GGT ACC CGG TTG AT-3'), and its complementary sequence (5'-SH-(CH₂)₆-TAC CCG CCC TCC TCC C-3') was synthesized by Biochem Ltd. (Shanghai, China), as previously reported.²⁴

Preparation of Luminol-Functionalized AuNFs. Luminol-functionalized AuNFs were prepared by reducing chloroauric acid with luminol and chitosan. Briefly, 0.2 g of chitosan was dissolved in 50 mL of glacial acetic acid (2%, V/V); then, 1 mL of luminol reserve solution was added, followed by the addition of double distilled water to 95 mL. The mixture was heated to boiling under condensation and reflux conditions; then, 5 mL of chloroauric acid reserve solution (0.2%, w/w) was added quickly and the mixture was boiled under reflux conditions for 0.5 h. The prepared material was further stirred for approximately 20 min to cool to room temperature and then stored at 4 °C for later use.

Preparation of Aminoized Fe₃O₄ Magnetic Nanomaterials. The process of nanoferric tetroxide silanization was performed as described in the literature,²⁵ as follows: 100 mg of nanoferric tetroxide (20 nm) was dissolved in 400 mL of 75% ethanol, then 6 mL of ammonia was added, and the nanoferric tetroxide was evenly dispersed in the solution by ultrasonic treatment for 5 min. Ethyl orthosilicate ammonia solution (2 mL) was added to the nanoferric tetroxide solution as prepared above for 6 h at a speed of 200 rpm for magnetic separation, which was then washed twice with anhydrous ethanol, and the supernatant was discarded to obtain silanized nanoferric tetroxide.

Ethyl acetate [160 mL, with a 5% (volume ratio) water content] was placed in a 250 mL beaker, the pH of the alcohol

solution adjusted to 5 with glacial acetic acid, and then, 8 mL of 3-amino-propyl triethoxysilane was added to the solution while stirring at 200 rpm. The resulting precipitate was washed twice using the magnetic separation technique. After the precipitate was dried in an oven at 110 °C for 30 min, it was placed in a drying dish to obtain amino-modified silanized nanoferric tetroxide for later use.

Construction of the Signal Probe. The signal probe is a compound of luminol-AuNFs linked to the mercapto complementary sequence (cDNA). In the present study, the signal probe was assembled in accordance with the method described by Li and Cui.²⁶

First, 5 mL of luminol-AuNFs was centrifuged at 10 000 rpm for 10 min, after which the supernatant was discarded, and the precipitated nanoparticles then dispersed in 1.5 mL of Tris-HCL buffer (30 mmol/L, pH 7.4) to obtain a luminol-AuNFs colloidal solution. A total of 60 μ L of 2.5 μ mol/L aptamer complementary sequence for LM was incubated with 30 μ L of 2.5 μ mol/L TCEP and shaken at 25 °C for 30 min; then, the above-mentioned luminol-AuNFs colloidal solution was added, incubating with slow agitation for 20 h. The precipitate was centrifuged and washed three times with PBS (0.01 mol/L, pH 7.4). Finally, the obtained signal probe (cDNA luminol-AuNFs) was dispersed in PBS for later use.

Construction of the Capture Probe. The capture probe is a compound of magnetic Fe₃O₄ nanomaterials attached to aptamers for LM, constructed using the conventional glutaraldehyde ligation technique.²⁷ First, magnetic Fe₃O₄ nanoparticles modified with avidin were prepared: To 5 mL of PBS, 5 mg of magnetic Fe₃O₄ nanomaterial was added, which was then fully dispersed by ultrasonication for 5 min, and 625 μ L of 25% glutaraldehyde solution was added. The mixture was thoroughly mixed and incubated at 37 °C for 2 h in the dark. PBS (5 mL) was added to the solid precipitate, and after ultrasonic dispersion, 20 μ L of avidin (1.0 mg/mL) was added and incubated for 12 h at 37 °C with slow oscillation. The supernatant was collected after the reaction, and the solid precipitate was washed several times to obtain avidin-based magnetic Fe₃O₄ nanoparticles. Second, through high specificity and strong affinity between biotin and avidin, the biotin-modified aptamer of LM was attached to the avidin-modified Fe₃O₄ MNPs. The steps of the procedure are as follows: the avidin-modified MNPs were added to 5 mL of PBS and then a specific quantity of biotinylated aptamer was added. After incubating on a shaker at 37 °C for 12 h, the unreacted aptamer was removed by magnetic separation. Finally, the capture probes were dispersed in 1 mL of PBS.

Determination of LM. First, 0.2 mL of capture probe and 0.2 mL of signal probe were incubated with a series of different concentrations of LM at 37 °C for 40 min. Magnetic separation was used to remove the combined LM and signal probe, and then, 0.5 mL of unbound signal probe was used for CL intensity detection. The CL curve of the system was determined after 1 min. The mean value of CL intensity between 400 and 500 s was selected for analysis of the experimental results.

Determination of Spiked LM in Milk Samples. Milk samples were selected to evaluate the reliability of the proposed method. The milk samples were purchased from local supermarkets and stored at 4 °C; LM was prepared and then added to 25 mL of sterile milk samples, respectively, where the final concentrations of LM were 1×10^1 CFU·mL⁻¹, 1×10^3 CFU·mL⁻¹, and 1×10^5 CFU·mL⁻¹, respectively. Milk

without bacterial solution was used as blank control. The mixed solution of the signal probe and capture probe was added to the milk sample with LM and the blank control, respectively. After incubation, magnetic separation was conducted, in which the upper liquid contained the competing signal probe. The more the LM, the more the signal probe. So, by measuring the electrochemical signal strength, the concentration of LM could be quantitatively analyzed and each sample was tested three times by the above method.

AUTHOR INFORMATION

Corresponding Authors

Weidan Chang – School of Food and Bioengineering, Henan University of Animal Husbandry and Economy, Zhengzhou 450046, China; Email: cwd201088@163.com

Wentao Xu – Department of Nutrition and Health, China Agricultural University, Beijing 100083, China; orcid.org/0000-0002-8572-8257; Email: xuwentao@cau.edu.cn

Authors

Weifeng Chen – School of Food and Bioengineering, Henan University of Animal Husbandry and Economy, Zhengzhou 450046, China

Liwei Cui – School of Food and Bioengineering, Henan University of Animal Husbandry and Economy, Zhengzhou 450046, China

Yanyan Song – School of Food and Bioengineering, Henan University of Animal Husbandry and Economy, Zhengzhou 450046, China

Wei Chen – School of Food and Bioengineering, Henan University of Animal Husbandry and Economy, Zhengzhou 450046, China

Yuan Su – Department of Nutrition and Health, China Agricultural University, Beijing 100083, China

Complete contact information is available at: <https://pubs.acs.org/10.1021/acsoomega.1c03527>

Author Contributions

[#]W.C. and L.C. contributed equally to this work.

Notes

The authors declare no competing financial interest.

ACKNOWLEDGMENTS

This research was supported by the Science and Technology Project of Henan Province (No. 182102110303), the doctor start-up fund (No. 53000153), and the Science and Technology Project of Henan Province (No. 212102310259).

REFERENCES

- (1) Mikš-Krajnc, M.; Lim, H. S. Y.; Zheng, Q.; Turner, M.; Yuk, H. G. Loop-mediated isothermal amplification (LAMP) coupled with bioluminescence for the detection of *Listeria monocytogenes* at low levels on food contact surfaces. *Food Control* **2016**, *60*, 237–240.
- (2) Raudsepp, P.; Koskar, J.; Anton, D.; Meremäe, K.; Kapp, K.; Laurson, P.; Bleive, U.; Kaldmäe, H.; Roasto, M.; Püssa, T. Antibacterial and antioxidative properties of different parts of garden rhubarb, blackcurrant, chokeberry and blue honeysuckle. *J. Sci. Food Agric.* **2019**, *99*, 2311–2320.
- (3) Zhang, L.; Zeng, J.; Ma, D.; Cheng, J.; Zhang, H. Application and evaluation of loop-mediated isothermal amplification method for detecting of *Listeria monocytogenes* in food. *Chinese J. Prev. Med.* **2014**, *48*, 213–217.

- (4) Wachiralurpan, S.; Sriyapai, T.; Areekit, S.; Sriyapai, P.; Thongphueak, D.; Santiwatanakul, S.; Chansiri, K. A one-step rapid screening test of *Listeria monocytogenes* in food samples using a real-time loop-mediated isothermal amplification turbidity assay. *Anal. Methods* **2017**, *9*, 6403–6410.
- (5) Li, F.; Ye, Q.; Chen, M.; Shang, Y.; Zhang, J.; Ding, Y.; Xue, L.; Wu, S.; Wang, J.; Pang, R. Real-time PCR identification of *Listeria monocytogenes* serotype 4c using primers for novel target genes obtained by comparative genomic analysis. *LWT-Food Sci. Technol.* **2021**, *138*, No. 110774.
- (6) Ghasemian, A.; Nojoomi, F.; Heidari Abhari, M.; Fallah Mehrabadi, J. A multiplex real-time PCR technique for simultaneous detection of *Listeria monocytogenes* and *Streptococcus agalactiae* among asymptomatic pregnant women. *Rev. Med. Microbiol.* **2018**, *29*, 136–139.
- (7) Tang, M. J.; Zhou, S.; Zhang, X.; Pu, J.; Ge, Q.; Tang, X.; Gao, Y. Rapid and sensitive detection of *Listeria monocytogenes* by loop-mediated isothermal amplification. *Curr. Microbiol.* **2011**, *63*, 511–516.
- (8) Yushina, Y.; Makhova, A.; Zayko, E.; Bataeva, D. Loop-mediated isothermal amplification (LAMP) for rapid detection of *L. monocytogenes* in meat. *Potravinarstvo* **2019**, *13*, 800–805.
- (9) Wang, D.; Zhang, G.; Lu, C.; Deng, R.; Zhi, A.; Guo, J.; Zhao, D.; Xu, Z. Rapid detection of *Listeria monocytogenes* in raw milk with loop-mediated isothermal amplification and chemosensor. *J. Food Sci.* **2011**, *76*, 611–615.
- (10) Kim, K. T.; Murano, E. A.; Olson, D. G. Development of an enzyme-linked immunosorbent assay (ELISA) for analysis of listeriolysin O produced by *Listeria monocytogenes*. *J. Rapid Methods Autom. Microbiol.* **1993**, *2*, 189–201.
- (11) Xu, L.; Bai, X.; Bhunia, A. K. Current state of development of biosensors and their application in foodborne pathogen detection. *J. Food Prot.* **2021**, *84*, 1213–1227.
- (12) Chen, W. F.; Hu, L.; Liu, A. P.; Li, J. Q.; Chen, F. S.; Wang, X. H. Expression and characterization of single-chain variable fragment antibody against staphylococcal enterotoxin A in *Escherichia coli*. *Can. J. Microbiol.* **2014**, *60*, 737–743.
- (13) Zhao, H. Y.; Bian, S.; Yang, Y.; Wu, X. P. Chiroplasmonic assemblies of gold nanoparticles as a novel method for sensitive detection of alpha-fetoprotein. *Microchim. Acta* **2017**, *184*, 1855–1862.
- (14) Zhang, Z. F.; Cui, H.; Lai, C.; Liu, L. Gold nanoparticle-catalyzed luminol chemiluminescence and its analytical applications. *Anal. Chem.* **2005**, *77*, 3324–3329.
- (15) Suh, S. H.; Jaykus, L. Nucleic acid aptamers for capture and detection of *Listeria spp.* *J. Biotechnol.* **2013**, *167*, 454–461.
- (16) Ma, X.; Jiang, Y.; Jia, F.; Yu, Y.; Chen, J.; Wang, Z. An aptamer-based electrochemical biosensor for the detection of *Salmonella*. *J. Microbiol. Methods* **2014**, *98*, 94–98.
- (17) Shahdordizadeh, M.; Yazdian-Robati, R.; Ramezani, M.; Abnous, K.; Taghdisi, S. M. Aptamer application in targeted delivery systems for diagnosis and treatment of breast cancer. *J. Mater. Chem. B* **2016**, *4*, 7766–7778.
- (18) Sakyi, S. A.; Aboagye, S. Y.; Otchere, I. D.; Liao, A. M.; Caltagirone, T. G.; Yeboah-Manu, D. RNA aptamer that specifically binds to mycolactone and serves as a diagnostic tool for diagnosis of buruli ulcer. *PLoS Neglected Trop. Dis.* **2016**, *10*, No. e4950.
- (19) Wang, Y.; Bao, L.; Liu, Z.; Pang, D. Aptamer biosensor based on fluorescence resonance energy transfer from upconverting phosphors to carbon nanoparticles for thrombin detection in human plasma. *Anal. Chem.* **2011**, *83*, 8130–8137.
- (20) Li, Y.; Qi, H.; Peng, Y.; Yang, J.; Zhang, C. Electrogenerated chemiluminescence aptamer-based biosensor for the determination of cocaine. *Electrochem. Commun.* **2007**, *9*, 2571–2575.
- (21) Ma, T.; Liu, P. Magnetic nanomaterials in Chinese medicine chemical composition analysis and drug metabolism and its industry prospect and development path research. *J. Chem.* **2020**, *12*, 1–8.
- (22) Hushiaran, R.; Yusof, N. A.; Abdullah, A. H.; Ahmad, S. A. A.; Dutse, S. W. Facilitating the indirect detection of genomic DNA in an electrochemical DNA biosensor using magnetic nanoparticles and DNA ligase. *Anal. Chem. Res.* **2015**, *6*, 17–25.
- (23) Bruno, J. G.; Richarte, A. M.; Phillips, T.; Savage, A. A.; Sivils, J. C.; Greis, A.; Mayo, M. W. Development of a fluorescent enzyme-linked DNA aptamer-magnetic bead sandwich assay and portable fluorometer for sensitive and rapid leishmania detection in sandflies. *J. Fluoresc.* **2014**, *24*, 267–277.
- (24) Ohk, S. H.; Koo, O. K.; Sen, T.; Yamamoto, C. M.; Bhunia, A. K. Antibody-aptamer functionalized fibre-optic biosensor for specific detection of *Listeria monocytogenes* from food. *J. Appl. Microbiol.* **2010**, *109*, 808–817.
- (25) Gu, J. Study on adsorption and chemical degradation of PFOS in water by amination nanometer iron tetroxide; Harbin Institute of Technology: Harbin, **2015**, *12*, 10–13.
- (26) Li, F.; Cui, H. A label-free electrochemiluminescence aptasensor for thrombin based on novel assembly strategy of oligonucleotide and luminol functionalized gold nanoparticles. *Biosens. Bioelectron.* **2013**, *39*, 261–267.
- (27) Hun, X.; Zhang, Z. Functionalized fluorescent core-shell nanoparticles used as a fluorescent labels in fluoroimmunoassay for IL-6. *Biosens. Bioelectron.* **2007**, *22*, 2743–2748.
- (28) Yang, X.; Zhou, X.; Zhu, M.; Xing, D. Sensitive detection of *Listeria monocytogenes* based on highly efficient enrichment with vancomycin-conjugated brush-like magnetic nano-platforms. *Biosens. Bioelectron.* **2017**, *91*, 238–245.